ISSN: 2688-8645

Research on Capacity Allocation of Wind-Solar-hydrogen Storage Microgrid based on HOMER

Huanjun Yang

Electricity Sales Management Department, China Petroleum Electric Energy Co., Ltd., Daqing, China

Abstract

Due to the significant volatility of wind and photovoltaic power generation, they also exhibit significant disturbances during grid connection, resulting in a decrease in the utilization rate of renewable energy. As a new type of renewable energy, hydrogen energy has the advantages of clean and efficient, easy storage, and convenient transportation, which can be used as a secondary carrier to improve the utilization rate of renewable energy. Based on the HOMERPRO software, a grid connected microgrid system for wind, solar, and hydrogen storage has been built. Selecting a certain region in Northeast China, with the lowest net present value total cost as the objective function, this study investigates hydrogen production systems at different time periods, compares and analyzes various microgrid capacity configurations, and concludes that the economy and availability of wind and solar hydrogen storage systems are the strongest.

Keywords

Microgrid; Hydrogen Fuel Cell; HOMER; Multienergy Complementation.

1. Introduction

In recent years, with the continuous expansion of the power grid scale, the disadvantages of large power grids have become increasingly prominent. Fossil energy is gradually depleting due to huge energy demands. Over time, the energy utilization rate of traditional power systems has also decreased, making it increasingly difficult to meet the needs of users. To achieve the concept of sustainable development, the utilization and development of renewable energy have been growing vigorously[1].

At present, the large power grid remains the main power supply method in the power system, but it still has disadvantages. Therefore, Professor R.H. Lasseter from the University of Wisconsin - Madison in the United States proposed the concept of microgrids and integrated new types of renewable energy into them[2].

Sustainable and environmentally friendly renewable energy sources such as solar photovoltaics, wind energy, fuel cells, and hydrogen energy are the most important energy sources for building a strong economy. However, if renewable energy is used alone, it will be severely restricted [3]. The electricity generated by wind turbines and solar photovoltaics is directly affected by environmental factors. Due to the instability of wind power and photovoltaic power generation, there is often an excess of electricity, resulting in unnecessary waste. Hydrogen fuel cells have many advantages such as high efficiency, zero emissions, and flexible structure. The excess electricity can be used for electrolyzing water to produce hydrogen, which is converted into hydrogen fuel, greatly improving the economic efficiency of the system.

This paper uses HOMERPRO software to simulate a park in Northeast China. It respectively discusses the rationality of hydrogen production at different time periods, and focuses on the coordinated capacity configuration, economy, and practicality of wind power, photovoltaics, hydrogen fuel cells, and energy storage units.

2. System Output Model and Objective Function

2.1. System Structure

The structure of the wind-solar-hydrogen-storage complementary microgrid system studied in this paper is shown in Figure 1.

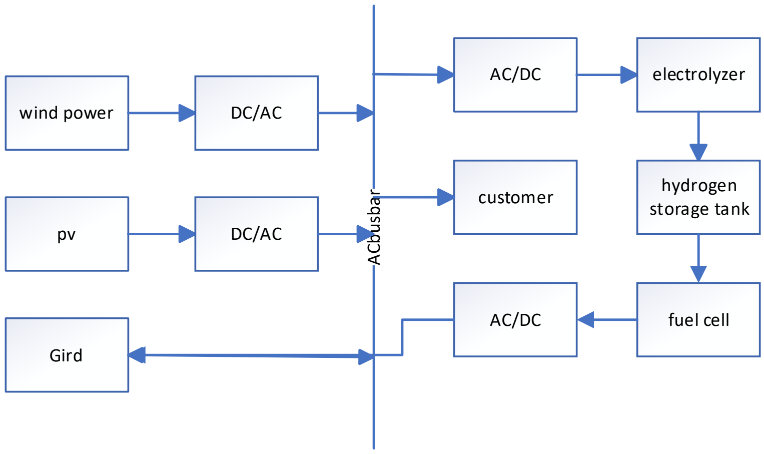

Figure 1. Structure Diagram of the Wind-Solar-Hydrogen-Storage Complementary Microgrid System

The wind turbines and photovoltaic arrays are connected to the DC bus via corresponding equipment. On the premise of ensuring economy and practicality, the power generation of renewable energy is maximally absorbed. Considering the inherent instability and intermittency of renewable energy, the energy storage system plays a crucial role in stabilizing output power fluctuations and improving power quality. The use of a single energy storage system may lead to instability factors in the energy storage system, such as short - term energy storage characteristics [4]. Therefore, a hydrogen storage module is introduced to convert the surplus electricity generated by renewable energy into the kinetic energy for electrolyzing water to produce hydrogen. The hydrogen storage module can not only solve the short - term energy storage problems that occur in single energy storage, but also improve the energy utilization rate of the system. The hydrogen fuel cell uses the hydrogen stored from electrolyzing water to produce hydrogen as fuel, forming a cyclic system to enhance economic benefits.

2.2. Wind Turbine Output Model

Based on the wind - solar - hydrogen - storage system, a system model integrating wind turbines, photovoltaic arrays, hydrogen fuel cells, hydrogen storage, and batteries is constructed.

Wind turbine output model [5]:

$$\begin{cases} 0 & v \le v_1 \\ \dfrac{P}{v_r^3 - v_1^3} v^3 - \dfrac{P}{v_r^3 - v_1^3} v_1^3 & v_1 \le v \le v_r \\ P & v_r \le v \le v_2 \\ 0 & v \ge v_2 \end{cases} \tag{1}$$

ISSN: 2688-8645

$$P = \frac{1}{2}\rho S C_p v^3 \eta_x \quad (2)$$

Among them:
(P)represents the output electrical power of the wind turbine, with the unit of watt(W)
(ρ)represents the air density, with the unit of kilogram per cubic meter (kg/m^3)
(S)represents the area of the wind turbine blades, with the unit of square meter (m^2)
(C_P)represents the power coefficient of the wind turbine. It usually ranges from 0 to 1 and indicates the efficiency of the wind turbine in obtaining energy from the wind.
(v)represents the wind speed, with the unit of meter per second (m/s)
(η_x)represents the power transmission efficiency.
(v_1)(v_2)(v_r)represent the cut - in wind speed, cut - out wind speed, and rated wind speed respectively, with the unit of meter per second(m/s).

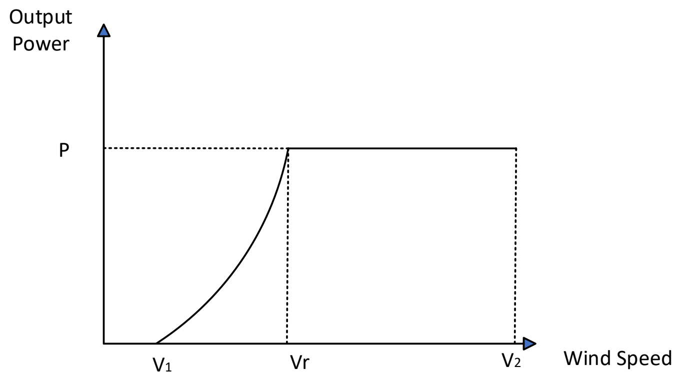

Figure 2. Output power curve of the wind turbine

This model basically describes the relationship between the output of the wind turbine and the wind speed, blade area, air density, and power coefficient. It should be noted that the actual output of the wind turbine is also affected by other factors, such as mechanical losses and generator efficiency. However, the above - mentioned model provides a basic framework for estimating the output of the wind turbine.

In practical applications, the power generation efficiency of wind turbines is reduced due to different losses from various factors, including availability loss, wake effect loss, turbine performance loss, electrical loss, environmental loss, derating loss, and other losses. The mathematical expression for the total loss is:

$$L_w = \prod_{i=1}^{n} 1 + \frac{L_i}{100} \quad (3)$$

Among them: Each loss percentage is an L_i.ranging from L_1 (availability loss) to L_7 (other losses). Then, the power output of the turbine is scaled down proportionally according to the obtained coefficient.

2.3. Photovoltaic Output Model

Photovoltaic panels have different power output efficiencies under different environmental factors, which are usually related to illumination intensity, air temperature, illumination index, environmental pollution, etc. The following three models are common photovoltaic panel output models:

(1)Idealized Photovoltaic Panel Model:

$$P = IV \quad (4)$$

Among them: P is the output power value. V is the voltage value of the photovoltaic panel. I is the current value of the photovoltaic panel.

This model is usually used for simplified calculations and does not consider practical effects such as the internal resistance of the battery.

(2) Single-Diode Equivalent Circuit Model:

This model takes into account the use of a single diode to reflect the characteristics of the photovoltaic panel. Its voltage-current characteristic model is:

$$I = I_{ph} - I_{01} \cdot \left(e^{\frac{q(V+IR)}{nKT}} - 1 \right) \tag{5}$$

Among them: I_{ph} is the current induced by illumination. I_{01} is the reverse saturation current. R is the equivalent series resistance of the photovoltaic panel. V is the voltage value and $I$is the current value. This model introduces the reverse saturation current and the internal resistance of the battery, restoring the power generation efficiency of the photovoltaic panel in actual situations to a certain extent.

(3) C-P&R Model:

$$Y_{(\tau)}(t) = Y\left(\frac{I_0}{Y_0}\right)\left(a_3 + b_3 \cos\omega_t\right) \tag{6}$$

Among them: Y is the total amount of solar radiation. I_0 is the hourly radiation on the horizontal plane outside the atmosphere. Y_0 is the daily total radiation on the horizontal plane outside the atmosphere. ω_t is the hour angle at the midpoint of 1 hour [6].

$$\begin{cases} a_3 = 0.409 + 0.5016\sin\left(\omega_s - 60^\circ\right) \\ b_3 = 0.6609 + 0.4767\sin\left(\omega_s - 60^\circ\right) \\ I_0 = I_{SC} E_0 \cos\delta \cos\phi\left(\omega_s - \omega_t\right) \end{cases} \tag{7}$$

Among them: I_{SC} is the sunset hour angle, and $\omega_s = \frac{\pi}{12}(t-12)$. \$I_{SC}\$ is the solar constant, with a value of $4.921\mathrm{MJ/(m^2 \cdot h)}$. $\mathrm{E_0}$ is the earth eccentricity correction coefficient, and $\mathrm{E_0} = 1 + 0.033\cos\frac{2\pi n}{365}$, where n is the number of days in a year. δ is the solar declination angle, and $\phi$is the geographical latitude.

$$P_{pv}(t) = f_{pv} P_{STC} \frac{G_c(t)}{G_{STC}}\left[1 + k\left(T_c(t) - T_{STC}\right)\right] \tag{8}$$

Among them: f_{pv} is the derating coefficient, which is related to the parameters of the photovoltaic power generation system. The derating coefficients of devices with different parameters are different. P_{STC} is the rated output power under standard conditions, with the unit of (KW). $G_c(t)$ is the actual irradiance, with the unit of $(\mathrm{KW/m^2})$. G_{STC} is the irradiance under standard conditions, with the unit of $(\mathrm{KW/m^2})$. k is the power temperature coefficient, with the unit of (%/°C). $T_c(t)$ is the surface temperature of the photovoltaic panel at time t, with the unit of (°C). T_{STC} is the actual temperature of the photovoltaic panel under standard conditions.

Comparing the three photovoltaic power generation output models, the idealized photovoltaic panel model is too simplified and does not conform to the actual power generation situation. The single-diode equivalent circuit model only takes into account the limiting factors of the photovoltaic panel itself and is not sufficient to simulate the real situation. In this paper, the C-P&R model is selected for research. Since the HOMERPRO software is used for simulation and

ISSN: 2688-8645

the illumination resources for 8,760 hours in a year are difficult to predict, it is more reasonable to use historical data as a reference and calculate the radiation value by using the C-P&R model.

2.4. Energy Storage Model

Due to the high rate of curtailed electricity in clean energy power generation, in this paper, the surplus electricity during the off-peak power consumption periods and the non-heating periods is utilized to produce hydrogen through water electrolysis, and the hydrogen is stored in hydrogen storage tanks.

The Hydrogen Production Model of the Alkaline Electrolyzer [7]:

$$P_c = U_0 I_c + \frac{\alpha}{A_c} I_c^2 + \beta \log\left(\frac{T_c}{A_c} I_c + 1\right) I_c \tag{9}$$

Among them: P_c is the power of the electrolyzer, with the unit of (KW). U_0 is the reversible voltage, with the unit of (V). I_c is the electrolyzer current, with the unit of (A). T_c is the electrolyzer temperature, with the unit of (°C). α and β are the ohmic resistance parameter of the electrolyte and the electrode over - voltage coefficient respectively. A_c is the effective area of the electrolyzer, with the unit of (m^2).

Autonomous model of the hydrogen storage tank:

$$A_{ht} = \frac{Y_{ht} LHV_{H_2}}{L_{prim,ave}} \tag{10}$$

Among them: Y_{ht} is the capacity of the hydrogen storage tank, with the unit of (kg). LHV_{H_2} is the energy content of hydrogen, with the unit of (MJ/kg) $L_{prim,ave}$ is the average primary load, with the unit of (kWh/d).

Hydrogen consumption rate of the fuel cell [7]:

$$Q_{H_2 fc,t} = \frac{N_{fc} P_{fc,t}}{V_{stack,tZF}} \tag{11}$$

Among them: N_{fc} is the number of single fuel cells connected in series. $P_{fc,t}$ is the power of a single fuel cell in the time period t. $V_{stack,t}$ is the stack voltage of the fuel cell in the time period t. z is the number of electron transfers per reaction. F is the Faraday constant.

Efficiency of the hydrogen fuel cell:

$$\eta = P_{out} / Q_{in} \tag{12}$$

Among them: η is the efficiency of the hydrogen fuel cell. P_{out} is the output power. Q_{in} is the average total input power to the power generation system.

Autonomous model of the battery pack:

$$A_{batt} = \frac{N_{batt} V_{nom} Q_{nom} \left(1 - \frac{q_{\min}}{100}\right)}{L_{prim,ave}} \tag{13}$$

Among them: N_{batt} is the number of batteries in the battery pack. V_{nom} is the nominal voltage of a single battery, with the unit of (V). Q_{nom} is the nominal capacity of a single battery, with the unit of (Ah). q_{min} is the minimum state of charge of the battery pack, with the unit of (%). $L_{prim,ave}$ is the average primary load, with the unit of (kWh/d).

2.5. Objective Function

The net present value of the total cost of the microgrid, and its formula is:

$$F_{\min} = C_{ca} + C_{re} + C_{O\&M} + C_{be} - C_{sa} \tag{14}$$

ISSN: 2688-8645

Among them: C_{ca} is the purchase cost. C_{re} is the replacement cost. $C_{O\&M}$ is the operation and maintenance cost. C_{be} is the penalty term for energy waste. C_{sa} is the depreciation cost when replacing equipment.

The curtailment rate of the system, and its formula is:

$$\omega_{\min} = \frac{\sum E_{ex}}{\sum E_p} \tag{15}$$

Among them: E_{ex} is the total excess electricity (kWh/yr), and E_p is the total generated electricity (kWh/yr).

2.6. Constraints

Taking into account the safety of the entire microgrid system and the service life of the entire battery pack, the relationship between the state of charge (SOC), battery charging power, and battery discharging power is as follows:

$$SOC^{MIN} \le SOC^{\tau} \le SOC^{MAX} \tag{16}$$

$$0 \le P(t) \le \min\left\{ p_{\max}^{c}, \frac{E_{bN}\left[SOC^{MAX} - SOC(t-1)\right]}{\Delta t \eta_c} \right\} \tag{17}$$

$$0 \le P(t) \le \min\left\{ p_{\max}^{d}, \frac{E_{bN}\left[SOC(t-1) - SOC^{MIN}\right]\eta_d}{\Delta t \eta_c} \right\} \tag{18}$$

Among them, SOC^{MIN} and SOC^{MAX} are the minimum and maximum values of the state - of - charge (SOC) of the battery respectively. P_{max}^{c} is the maximum rated continuous charging power of the battery pack, and P_{max}^{d} is the maximum rated continuous discharging power of the battery pack. E_{bN} is the rated capacity of the battery pack. η_c and η_d represent the charging and discharging efficiencies of the battery pack respectively. In the HOMER software, the operating range of the SOC of the battery pack is set to 0.4 - 0.95.

System power balance constraint:

$$P_T^{PV} + P_T^{wind} + P_T^{gird} + P_T^{BA} + P_T^{H_2} = 0 \tag{19}$$

Among them, P_T^{PV}、P_T^{wind}、P_T^{gird}、P_T^{BA}、 and $P_T^{H_2}$ are the active power of the photovoltaic system, the active power of the wind turbine system, the power exchanged with the power grid, the charging - discharging power of the battery pack, and the charging - discharging power of the hydrogen fuel cell within the time period T, respectively.

3. Simulation Model

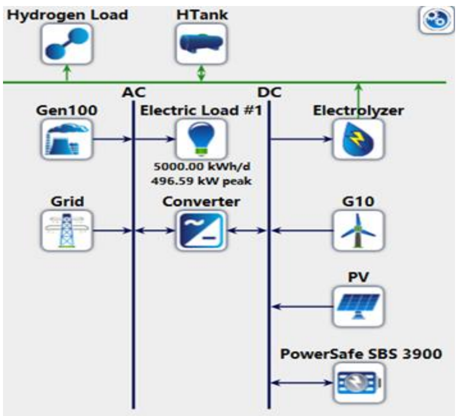

Figure 3. Simulation diagram of the wind - solar - hydrogen - storage system

A region in Northeast China is selected as the research model in this paper. A hybrid energy model of wind, solar, and hydrogen is built using HOMEPRO software. Figure 3 shows the system simulation diagram built in the HOMER software.

In this model, the wind turbines, photovoltaic panels, and battery packs are connected to the DC bus. The AC section consists of a hydrogen fuel cell, which is connected via a bidirectional converter. This setup enables the conversion between AC and DC power and the charging and discharging of the batteries. The system has an operating period of 20 years, with a component discount rate of 8% and an inflation rate of 2%.

3.1. Wind and Solar Resources

The wind and solar resource data are selected according to the HOMER software. The data sources are NASA and the National Renewable Energy Laboratory. The geographical location is set at 46° 35.7' N, 125° 8.5' E. The local area is rich in wind and solar resources, and the annual average wind speed is approximately 5.98 m/s. Through the analysis of the Weibull distribution data, the scale parameter K is set to 2, and the aurora - related factor value is set to 0.85. The monthly average wind speeds obtained by fitting are shown in Table 1.

Table 1. Monthly wind and solar resources

Month	Clearness Index	Average Daily Solar Radiation ($kWh/m^2/day$)	Monthly average wind speed (m/s)
1	0.598	1.862	5.280
2	0.625	2.853	5.740
3	0.593	3.995	6.530
4	0.558	5.065	7.300
5	0.559	6.047	6.910
6	0.533	6.173	5.760
7	0.504	5.641	5.110
8	0.538	5.228	5.200
9	0.569	4.282	5.940
10	0.579	3.009	6.360
11	0.560	1.922	6.110
12	0.537	1.446	5.490

Using the HOMER software, the wind and solar resource data can be dispersed into 8760 hours [8]. The hourly data of the photovoltaic panels are shown in Figure 4, and the hourly wind speed data are shown in Figure 5.

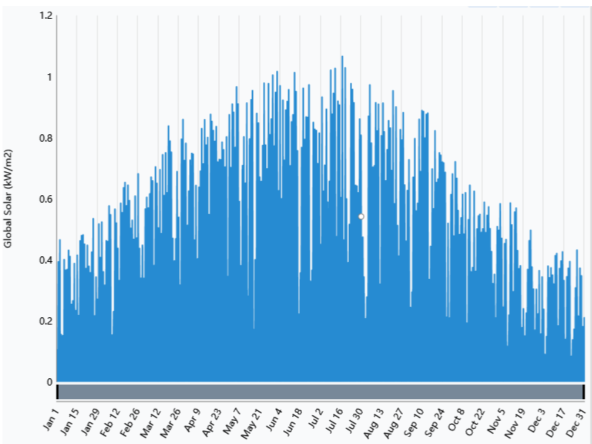

Figure 4. Hourly solar radiation on photovoltaic panels throughout the year

ISSN: 2688-8645

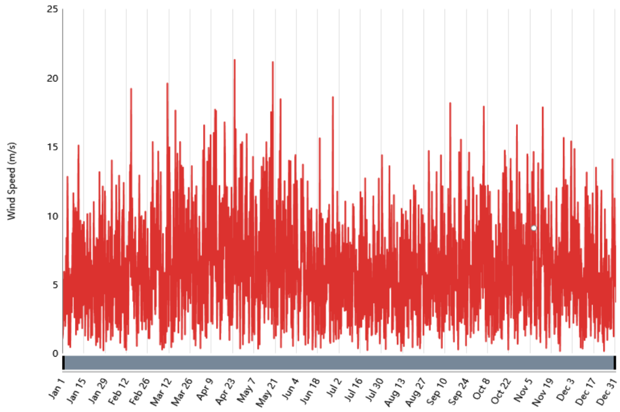

Figure 5. Hourly wind speed throughout the year

3.2. Analysis of Electricity Load Schemes

The annual load data of the users is shown in Figure 6.

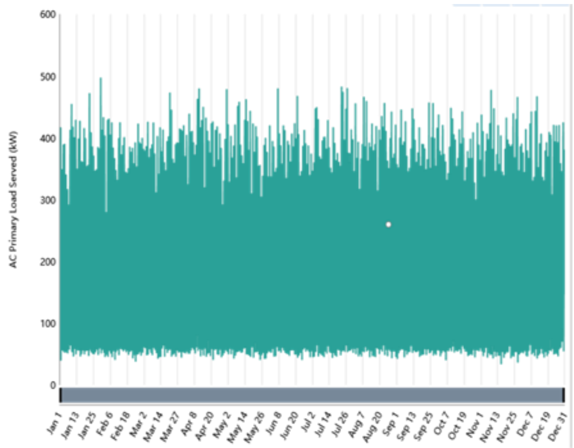

Figure 6. Annual load data of users

Scheme 1

The research location in this paper is set in a certain area in Northeast China. The months of January, February, November, and December are the heating periods, which are also the peak electricity - consumption periods. Based on the analysis of the wind - solar - hydrogen - storage system, during the non - heating periods, the electricity consumption of users is lower than that during the heating periods. The curtailed electricity during the non - heating periods is used as a resource for water electrolysis to produce hydrogen. The hydrogen load during the heating period is set to 0. If the hydrogen storage tank is full of hydrogen at this time, the system will stop producing hydrogen, achieving the effect of hydrogen production during the non - heating periods. The annual hydrogen load data is shown in Figure 7.

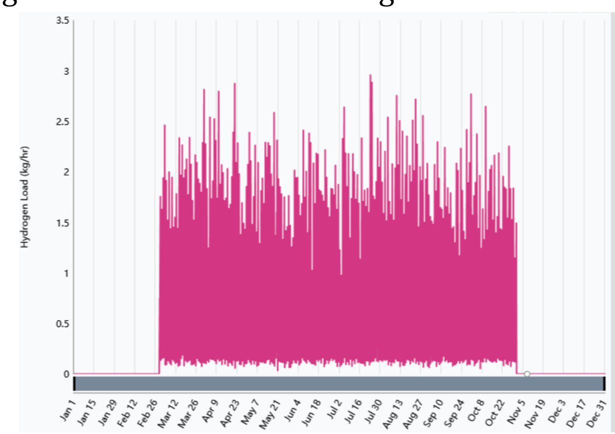

Figure 7. Annual hydrogen load data of Scheme 1

ISSN: 2688-8645

Scheme 2

Due to the impact of the global warming trend, the average summer temperature in northern China has also risen. Along with the improvement of the national economy, the use of cooling equipment such as air - conditioners in summer has become common in the north. As a result, July and August have also become peak electricity - consumption periods. Months of January, February, July, August, November, and December are regarded as the peak electricity - consumption periods throughout the year. Hydrogen production is carried out during the non - peak periods of other months. The annual hydrogen load data is shown in Figure 8.

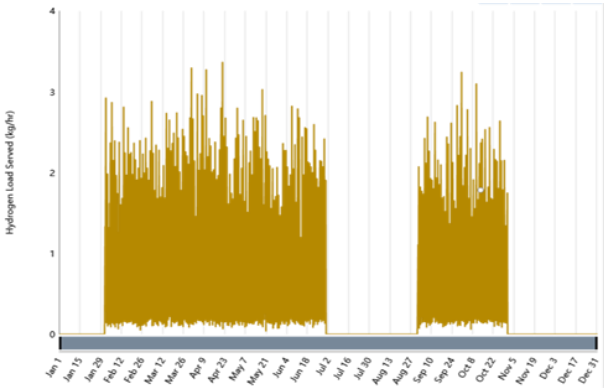

Figure 8. Annual hydrogen load data of Scheme 2

Scheme 3

Without considering time - segmented hydrogen production, the whole year is regarded as the hydrogen - production period. The annual load data is shown in Figure 9.

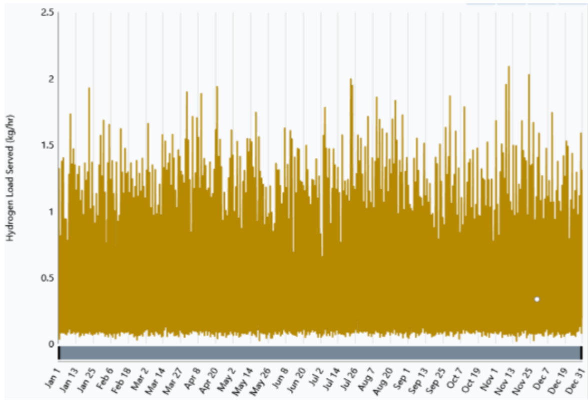

Figure 9. Annual hydrogen load data of Scheme 3

3.3. System Costs and Parameters

The system costs are shown in Table 2.

The corresponding parameter settings of the system are as follows: The system has an operating lifespan of 20 years. The discount rate for components is set at 8%, and the inflation rate is 2%. The derating factor of the photovoltaic panels is set to 0.2. The state - of - charge (SOC) of the battery is set within the range of 30% - 95%, which can extend the battery's service life. The efficiency of the converter is set at 90%. The operating hours of the electrolyzer are set during the daytime, specifically determined according to the different sunrise and sunset times of each month. The raw material price of the hydrogen fuel cell is set at 0.472 RMB/kg.

4. Simulation Result Analysis

The HOMERPRO software sorts the results in descending order according to the total net present value. There are two operating strategies: the load - following dispatch strategy (LF) and the cycle - charging strategy (CC). After inputting the relevant data for simulation, there are a total of six results, namely wind - solar - hydrogen - storage, solar - hydrogen - storage, wind - hydrogen - storage, wind - solar - hydrogen, wind - hydrogen, and solar - hydrogen. The specific results are shown in Table 3.

Table 2. Costs and service lives of each equipment

program	Initial cost (yuan/kW)	Replacement cost (yuan·kW)	maintenance cost (yuan/kW/year)	Service life (years)
Wind turbine	35000	35000	500	20
Photovoltaic panel	2500	2500	100	20
Battery	500	500	20	15
Converter	300	300	0	10
Electrolyzer	5000	4000	200	15
Hydrogen storage tank	500	500	0	20

Table 3. Capacity configurations of different types of microgrids

Model	Photovoltaic (kW)	Number of 10-kW wind turbines	Hydrogen fuel cell (kW)	Numberof batteries	Electrolyzer (kW)	Converter (kW)	Hydrogen storage tank (kg)
Wind - solar - hydrogen - storage	601	19	150	83	800	322	200
Solar - hydrogen - storage	858	0	150	53	800	176	200
Wind - hydrogen - storage	0	53	150	68	800	305	200
Wind - solar - hydrogen	203	42	150	0	800	372	200
Wind - solar - hydrogen	0	49	150	0	800	421	200
Solar - hydrogen	678	0	150	0	800	301	200

Table 4. Performance results of different types of microgrids

Model	Dispatch strategy	Electricity curtailment rate	Renewable energy penetration rate
Wind - solar - hydrogen - storage	LF	1.09%	54.5%
Solar - hydrogen - storage	LF	3.76%	47.2%
Wind - hydrogen - storage	LF	5.75%	46.8%
Wind - solar - hydrogen	CC	2.53%	50.7%
Wind - solar - hydrogen	CC	1.95%	45.2%
Solar - hydrogen	CC	4.30%	34.5%

As can be seen from Tables 3 and 4, the wind - solar - hydrogen - storage model is the most economical and has the highest reliability. Among them, the systems with energy - storage modules are more economical than those without energy - storage modules.

Based on the three schemes discussed in Section 2.2, a comparative analysis is carried out. The power generation is shown in Figures 10, 11, and 12.

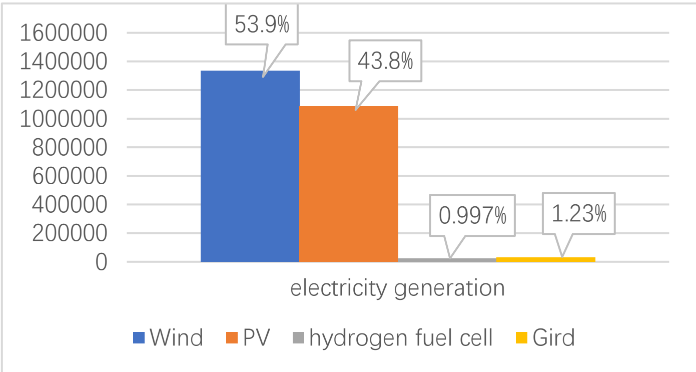

Figure 10. Power generation and proportion of each item in Scheme 1

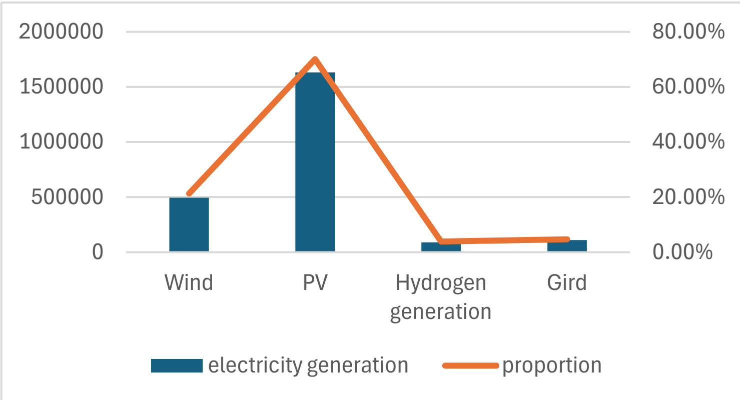

Figure 11. Power generation and proportion of each item in Scheme 2

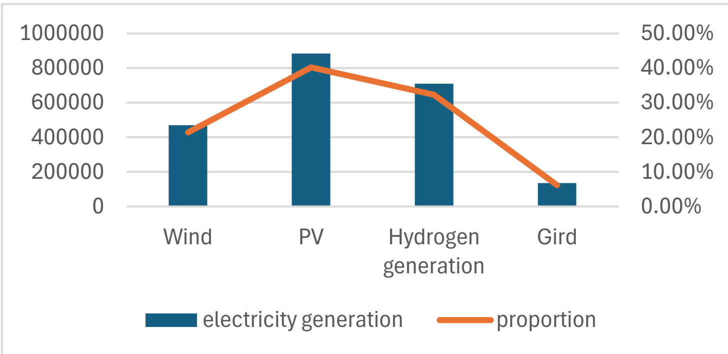

Figure 12. Power generation and proportion of each item in Scheme 3

Table 5. Comparison of results between the two schemes

Scheme	Electricity curtailment rate	NPC (10,000 yuan)	Renewable energy penetration rate	Hydrogen throughput (Kg)
1	6.23%	472	89.2%	27939
2	1.09%	460	54.5%	256350
3	6.05%	490	97.3%	7594

Figures 10, 11, 12 and Table 5 only discuss the wind - solar - hydrogen - storage model. Comparing the three schemes from the perspective of system reliability, Scheme 2 has higher reliability. The curtailment rate of Scheme 2 is 5.14% lower than that of Scheme 1 and 4.96% lower than that of Scheme 3. The curtailed electricity is reduced by 120,908 kWh and 125,865 kWh respectively compared with Scheme 1 and Scheme 3.

From the economic perspective, the total cost of Scheme 2 is slightly lower than that of Scheme 1 and Scheme 3. Although the utilization rate of renewable energy in Scheme 1 is much higher than that in Scheme 2, the actual throughput of hydrogen production and storage in Scheme 1 is far less than that in Scheme 2. The annual hydrogen usage in Scheme 1 is 27,939 kg, while in Scheme 2 it is 256,350 kg, and in Scheme 3 it is only 7,594 kg.

Considering the three schemes and six models comprehensively, the wind - solar - hydrogen - storage system has the highest economic efficiency and reliability when producing hydrogen during non - summer peak periods and non - heating periods.

5. Conclusion

In this paper, the HOMERPRO software is used to simulate the capacity configuration of the wind - solar - hydrogen - storage micro - grid model. A total of six models emerge. Through comparative analysis from the perspectives of economy and reliability, the superiority of the wind - solar - hydrogen - storage model is confirmed. Moreover, considering the environmental factors in Northeast China, hydrogen production is carried out during the off - peak power supply periods. This approach mitigates the issue of the inability to absorb a large amount of renewable energy, reduces the curtailed electricity of the system, and further optimizes the reliability and economy of the system.

References

[1] Yu Kaixuan. Research on the Optimal Configuration of Isolated Wind/Solar/Hydrogen/Storage Micro - Grid Based on MOBASDE Algorithm[D]. Taiyuan University of Technology, 2022.

[2] Lian Chao, Jiang Yijun, Chen Meng, et al. Research on the Power Supply Configuration of Micro - Grid Based on HOMER Simulation[C]//Zhejiang Electric Power Society, Shanghai Society of Electrical Engineering, Jiangsu Society of Electrical Engineering, Zhejiang Society of Electric Machinery and Power. Excellent Papers of Zhejiang Electric Power Society in 2013. China Electric Power Press, 2013: 6.

[3] Tian Cong. Research on the Optimization of Hybrid Energy Storage System Based on Wind and Solar Energy[D]. Jilin University, 2022.

[4] Chen Weirong, Fu Wangxuan, Han Ying, et al. Optimal Configuration of Wind - Solar - Hydrogen Multi - Energy Complementary Micro - Grid Considering the Demand Side[J]. Journal of Southwest Jiaotong University, 2021, 56(03): 640 - 649.

[5] Wang Kanhong, Zhao Zhengtong, Luo Jinghui. Two - Stage Optimal Matching Analysis of Wind - Solar - Hydrogen - Storage System[J]. Science Technology and Engineering, 2020, 20(26): 10790 - 10794.

[6] Luo Yun, Guo Yongxi, Yang Bo. Capacity Optimization Simulation of Wind - Solar - Biogas - Storage Micro - Grid Based on HOMER[J]. Hongshui River, 2018, 37(03): 37 - 41 + 45.

[7] Kong Lingguo. Research on the Optimal Configuration and Coordinated Control Strategy of Wind - Solar - Hydrogen Integrated Energy System[D]. North China Electric Power University (Beijing), 2017.

[8] Zuo Chong, Jia Yan, Mengkeqilao, et al. Research on the Optimal Capacity Configuration of Wind - Solar - Storage Complementary Power Generation System Based on HOMER Simulation[J]. Inner Mongolia Electric Power, 2023, 41(01): 21 - 25.